Study of photoisomerization of *azo* dyes in liquid crystals

D. Statman[a] and I. Jánossy
Research Institute for Solid State Physics and Optics, H-1525 Budapest, P.O. Box 49, Hungary

(Received 22 May 2002; accepted 22 November 2002)

The *trans-cis* isomerization of *azo* dyes in liquid crystalline hosts is studied. It is shown that the full set of parameters governing the isomerization process can be deduced from polarized pump–probe transmission measurements. The results indicate that the dye order parameter for the *trans* isomer is relatively high and is strongly related to the liquid-crystalline order. The *cis* isomer exhibits a much lower dye order parameter and is not strongly dependent on the liquid-crystalline phase. The barrier to the thermal *cis-trans* relaxation is found to be relatively unaffected by the liquid-crystalline phase, while changes are observed in the pre-exponential factor. © *2003 American Institute of Physics.* [DOI: 10.1063/1.1538598]

I. INTRODUCTION

The optical properties of absorbing liquid crystals have attracted considerable interest in the last several years. In particular, a number of intriguing light-induced effects has been found to occur in liquid crystals doped with, or consisting entirely of *azo* derivatives. For example, Ikeda and Tsutsumi[1] observed nematic-to-isotropic transition due to phototransformation of *azo* molecules. Chen and Brandy[2] reported self-diffraction effects in an *azo* dye doped nematic. Folks *et al.*[3] investigated photoinduced textural instabilities in a smectic liquid crystal containing an *azo*benzene derivative.[3] Barnik *et al.*[4] observed anomalous angular dependence of the optical torque in *azo* dye doped liquid crystals, which was explained by taking into account the photoisomerization of the dopant molecules.[5] Another interesting phenomenon connected with photoisomerization occurs in *azo*benzene side-chain liquid-crystalline polymers, where light-induced *trans-cis* transitions lead to the development of macroscopic anisotropy in initially optically isotropic systems.[6,7]

The quantitative interpretation of this phenomena requires the knowledge of the basic parameters of the photoisomerization process. These parameters include the absorption cross sections of the isomers, the quantum efficiencies of the light-induced *trans-cis* and *cis-trans* isomerizations, and the rate constant of the thermal *cis-trans* back relaxation. As we deal with uniaxial anisotropic media, the absorption cross sections have two independent components; one for an ordinarily polarized beam, and the other for the extraordinary beam. Thus, the complete characterization of the isomerization process requires, altogether, the determination of seven parameters.

One possible way to obtain these parameters is to investigate the light-induced reorientation process itself. The Risø group proposed such an approach for side-chain nematic polymers.[8–10] They used a mean-field theory to describe the time dependence of the light-induced birefringence in the mesogenic side-chain nematic polymers. From a comparison of theory with experiment, they determined, through a fitting procedure, the average cross sections for both the *trans* and *cis* isomers, as well as the quantum efficiencies of the light-induced transitions. This method, however, is restricted to systems where reorientation is easily observed. In addition, it does not give complete information for the relevant parameters.

In a paper, published in 1998,[11] we proposed an alternative approach, which is based on polarized pump–probe transmission measurements. Our method is applicable to guest–host systems, in which a small amount of an *azo*-dye dopant is added to well-oriented, monodomain liquid-crystalline hosts (typically to low-molecular mass liquid crystals). During the experiments, macroscopic reorientation does not take place. This condition can be ensured partly by choosing appropriate geometries and partly by keeping the pump and probe intensities at sufficiently low levels. Furthermore, the probe intensity is kept low enough, to avoid isomerization by its presence; transitions are only due to the pump beam.

Under the circumstances just outlined, transmission measurements of the probe beam alone can yield the ordinary and extraordinary *trans* absorption cross sections. Transmission measurements, performed with pump intensities high enough to saturate the *cis* concentration, allow for determining the *cis* absorption cross sections and the ratio of the quantum efficiencies. In order to get the absolute values of the quantum efficiencies, the probe transmission must be measured as a function of the pump intensity. Finally, the rate constant of the thermal *cis-trans* transitions can be obtained by observing the probe relaxation after the pump is switched off. Thus, all relevant parameters can be derived from the data, using standard rate equations only.

In the present article, we apply the procedure outlined herein to certain *azo* dyes. We selected dyes that can be useful in the nonlinear optical applications, mentioned in the first paragraph of Sec. I. They absorb strongly in the visible range, in particular at the wavelength 488 nm, at which the

[a]Permanent address: Department of Physics, Allegheny College, Meadville, PA 16335; electronic mail: dstatman@allegheny.edu

experiments were performed. The thermal *cis-trans* relaxation times for these substances are relatively short, ranging from a second to few milliseconds. This circumstance ensures a fast recovery of the initial state after the light is turned off.

The dyes were dissolved in two different liquid-crystalline hosts. The first host, octyl-cyano-biphenyl (8CB) exhibits smectic A, nematic and isotropic phases, while the second host is nematic throughout the temperature range investigated. One of our aims is to provide quantitative values of the parameters of photoisomerization in these specific guest–host systems. In addition, we intend to gain insight to the problem as to how these parameters are influenced by the arrangement of the surrounding solvent molecules. In the smectic phase, the host molecules possess both translational and orientational order; in the nematic phase only orientational order is present, while in the isotropic phase both types of order are absent. Therefore, measurements in 8CB should indicate the importance of the molecular order of the host material on the photoisomerization process. Measurements in the nematic host are carried out in the same temperature range as for 8CB, and serve as a comparison.

The article is organized as follows. In Sec. II, we review the theoretical description of photoisomerization in liquid crystals. In Sec. III, the experimental techniques are described. The results are presented and discussed in Sec. IV and conclusions discussed in Sec. V.

II. THEORETICAL DESCRIPTION

Consider a planar aligned liquid crystal system doped with trace amount of *azo* dye. The dye molecules can be made to isomerize via photoexcitation. Light-induced *trans-cis* and *cis-trans* transitions, as well as thermal relaxation of the *cis* isomer to *trans*, are the elementary processes involved in isomerization. For light normally incident on the sample, the optical field polarization can be resolved in terms of the ordinary component, that which is orthogonal to the liquid crystal director, and the extraordinary component, that which is parallel to the director. The fraction of *cis* isomers, X, is determined by the light polarization and intensity, and is described by

$$\frac{dX}{dt}=\sigma_T^i\Phi_{TC}\frac{I^i}{h\nu}(1-X)-\sigma_C^i\Phi_{CT}\frac{I^i}{h\nu}X-\frac{X}{\tau}, \tag{1}$$

where I^i is the light intensity, σ_C^i and σ_T^i are the absorption cross sections of the *cis* and *trans* isomers, respectively, for light of polarization i, Φ_{TC} and Φ_{CT} are the quantum efficiencies of the *trans-cis* and *cis-trans* transitions, respectively, and τ is the relaxation time back to steady state in the absence of light. The first and second terms on the right-hand side of Eq. (1) describe light-induced transitions, while the third term accounts for the thermal relaxation of the *cis* component.

Equation (1) can be rewritten in terms of a saturation intensity I_S as

$$\frac{dX}{dt}=\sigma_T^i\Phi_{TC}\frac{I^i}{h\nu}-\left(\frac{I^i}{I_S^i}+1\right)\frac{X}{\tau}, \tag{2}$$

where the saturation intensity, I_S^i, is given by

$$I_S^i=\left[\sigma_T^i\Phi_{TC}\left(1+\frac{\sigma_C^i\Phi_{CT}}{\sigma_T^i\Phi_{TC}}\right)\frac{\tau}{h\nu}\right]^{-1}. \tag{3}$$

From Eq. (2), the steady-state fraction of *cis* isomers is given by

$$X_{\mathrm{eq}}^i=\frac{X_S^i}{1+I_S^i/I^i}, \tag{4}$$

where the saturation *cis* fraction is

$$X_S^i=\frac{(\Phi_{TC}/\Phi_{CT})}{(\sigma_C^i/\sigma_T^i)+(\Phi_{TC}/\Phi_{CT})}. \tag{5}$$

From Eqs. (4) and (5), it is clear that the saturation intensity, I_S^i, and the saturation *cis* fraction, X_S^i determine the steady-state fraction of the *cis* isomer. The latter is determined by the ratio of *cis* and *trans* absorption cross sections, σ_C^i/σ_T^i, and the ratio of the quantum efficiencies, Φ_{TC}/Φ_{CT}.

One technique for determining these parameters is that of pump probe in which an *m*-polarized probe beam tests the absorbance changes caused by an *i*-polarized pump beam at the same wavelength. In the absence of illumination, when only *trans* isomers are present, the probe beam experiences an absorption coefficient $\alpha_T^m=N\ \sigma_T^m$, with N being the total number density of dye molecules. The measurement of the absorbances $A_T^m=\alpha_T^m L$ (L is the sample thickness) under such circumstances allows for the determination of the *trans* absorption cross sections.

In the presence of the pump, the absorption coefficient can be assumed to be a linear superposition of the contributions from the two isomers:

$$\alpha^m=\alpha_T^m(1-X)+\alpha_C^m X, \tag{6}$$

where $\alpha_C^m=N\ \sigma_C^m$ is the *cis* absorption coefficient. When the pump beam is much higher than the saturation intensity, the *cis* fraction is equal to the saturation value X_S^i, given by Eq. (4). The saturated absorbances in this case are given by

$$A_s^{im}=(1-D^m X_S^i)A_T^m, \tag{7}$$

with

$$D^m=1-\frac{\sigma_C^m}{\sigma_T^m}. \tag{8}$$

As shown in Ref. 11, measuring the saturated probe absorbances at various combinations of ordinary and extraordinary light for the pump and probe, respectively, together with the two A_T^m values, allows for the determination of the ratios σ_C^i/σ_T^i and Φ_{TC}/Φ_{CT}:

$$\frac{\Phi_{TC}}{\Phi_{CT}}=\left(\frac{A_T^m-A_s^{ee}}{A_s^{ee}-A_s^{oe}}\right)\left(\frac{A_s^{oe}}{A_T^e}-\frac{A_S^{oo}}{A_T^o}\right), \tag{9a}$$

$$\frac{\sigma_C^i}{\sigma_T^i}=\frac{A_s^{ii}\left(\frac{\Phi_{TC}}{\Phi_{CT}}\right)}{A_T^i\left(\frac{\Phi_{TC}}{\Phi_{CT}}\right)-A_S^{ii}}. \tag{9b}$$

With the help of these ratios, one can also calculate the X^i and D^i values, according to Eqs. (5) and (8), respectively.

In order to determine the saturation intensities, measurements at intermediate pump intensities, with incomplete *cis* saturation, must be carried out. In this situation, the steady-state attenuation of the probe and pump beams along the sample normal (z direction) are described by the equations, respectively:

$$\frac{dI^m}{dz} = -\alpha^m I^m = -\alpha_T^m (1 - D^m X_{\mathrm{eq}}^i) I^m, \tag{10a}$$

$$\frac{dI^i}{dz} = -\alpha^i I^i = -\alpha_T^i (1 - D^i X_{\mathrm{eq}}^i) I^i. \tag{10b}$$

Equations (10a) and (10b) can be integrated, leading to the following expression for the probe absorbance (see Appendix):

$$A^{im} = -\ln \frac{I^m(L)}{I^m(0)} = A_T^m + \frac{A_T^m}{A_T^i} \frac{D^m X_S^i}{1 - D^i X_S^i} \times \ln\left[\frac{I_S^i/I^i(0) - (D^i X_S^i - 1) I^i(L)/I^i(0)}{I_S^i/I^i(0) - (D^i X_S^i - 1)} \right]. \tag{11}$$

This expression contains also the pump transmission, $I^i(L)/I^i(0)$. For pump and probe beams of the same polarization, propagating colinearly, the *i*-polarized pump is attenuated by the same amount as the *i*-polarized probe. Hence, one has $I^i(L)/I^i(0) = -\ln A^{ii}$. Furthermore, if we take D^i and X^i as known parameters from the measurements with saturated *cis* concentration, Eq. (11) can be considered to be a transcendental equation for $I_S^i/I^i(0)$. This can be readily solved numerically. In a more precise method, the probe absorbance is measured as a function of pump intensity (therefore giving the pump absorbance, as well), then the saturation intensity can be determined by numerically varying it so as to minimize the difference between the left- and right-hand sides of Eq. (11).

The saturation intensity can be obtained also by measuring the transient relaxation time as a function of the intensity. This possibility will be discussed in a future paper.

The thermal relaxation time can be determined by observing the decay of the probe intensity after the pump is switched off. From the values of I_S^i and τ, the absolute values of the quantum efficiencies can be determined [c.f. Eq. (3)]. Thus, we demonstrated that in liquid crystals, the full set of parameters governing the isomerization process can be deduced from polarized transmission measurements.

It is interesting to note that this procedure breaks down for the isotropic phase. In this phase, only four independent quantities can be inferred from the data, namely the linear and the saturated absorbance, the saturation intensity, and the thermal relaxation time. The model contains, however, five parameters for the isotropic phase: the *trans* and *cis* absorption cross sections, the two quantum efficiencies, and the thermal relaxation time. Hence, to obtain all parameters in the isotropic phase, one has to use some assumption not based on direct measurements. On the other hand, this method can be applied without any modification to smectic phases. Therefore, demonstrating certain advantages when compared with the procedure applied by the Risø group. Their approach requires light-induced director reorientation, which is hard to realize in smectic mesophases.

III. EXPERIMENT

The dyes investigated were disperse orange 3 (DO3), disperse red 13 (DR13) from Aldrich, and methyl red from Merck. The hosts were 8CB and the eutectic mixture E63, supplied by British Drug House. The samples prepared were DR13 in 8CB (0.1% wt%), DR13 in E63 (0.1% wt%), DO3 in 8CB (0.4% wt%), DO3 in E63 (0.47% wt%), methyl red in 8CB (0.1% wt%) and methyl red in E63 (0.06% wt%). Planar aligned liquid crystal samples were prepared in the usual way. Glass slides were spincoated with polyamic acid, which was heated in an oven to form a coating of polyimide, and then rubbed with velvet in the preferred direction. Each cell was 50 μm thick, set by a pair of spacers.

A schematic of the pump–probe experiment is shown in Fig. 1. The pump was an Ar^+ laser tuned to the 488 nm line. Saturation measurements were made by setting the intensity of the pump high enough to saturate the dye, but not high enough to heat the liquid crystal significantly. The polarized pump beam was directed though a computer-controlled twisted nematic cell, which set the polarization of the beam, and a computer-controlled shutter. The unfocused pump beam was then directed through the liquid crystal sample. A beam splitter was used to direct a portion of the pump beam to a detector to measure the incident pump intensity. The probe was from a second much weaker Ar^+ laser also tuned to the 488 nm line and made a small angle (few degrees) with the pump. The polarized probe was also directed through a computer-controlled shutter and twisted nematic cell. Care was taken to make sure that overlap between the pump and probe beams within the sample were optimized. The unfocused probe was then directed to a photodetector. The output of the photodetector was sent to a storage oscilloscope. The liquid crystal cell was placed in a holder with external temperature control.

For the dyes methyl red and DO3, the linear absorbances (i.e., probe absorbance in the limit of zero intensity), the nonlinear absorbances, and relaxation time were measured by sequencing the shutters and twisted nematics as follows. For either ordinary or extraordinary probes, the probe shutter was opened. The transmitted probe was observed to increase in intensity, indicating that even at the low pump intensities there was some *cis-trans* isomerization. The initial intensity was taken as the linear absorbance, A_{Tm}. With the twisted nematic set for *o* pump, the pump shutter was then opened. After the probe intensity reached the new steady-state value, the pump shutter was closed allowing for relaxation of the probe. With the twisted nematic now set for *e* pump, the pump shutter was again opened, and the probe reached the new steady-state intensity. The pump shutter was closed again. After the probe signal relaxed back to the no-pump steady-state intensity, the probe shutter was closed. Figure 2 shows typical measurements of this sequence. Background measurements were also taken, with the probe blocked, to make sure that any scattering of the pump into the probe detector was minimal and, if necessary, accounted for.

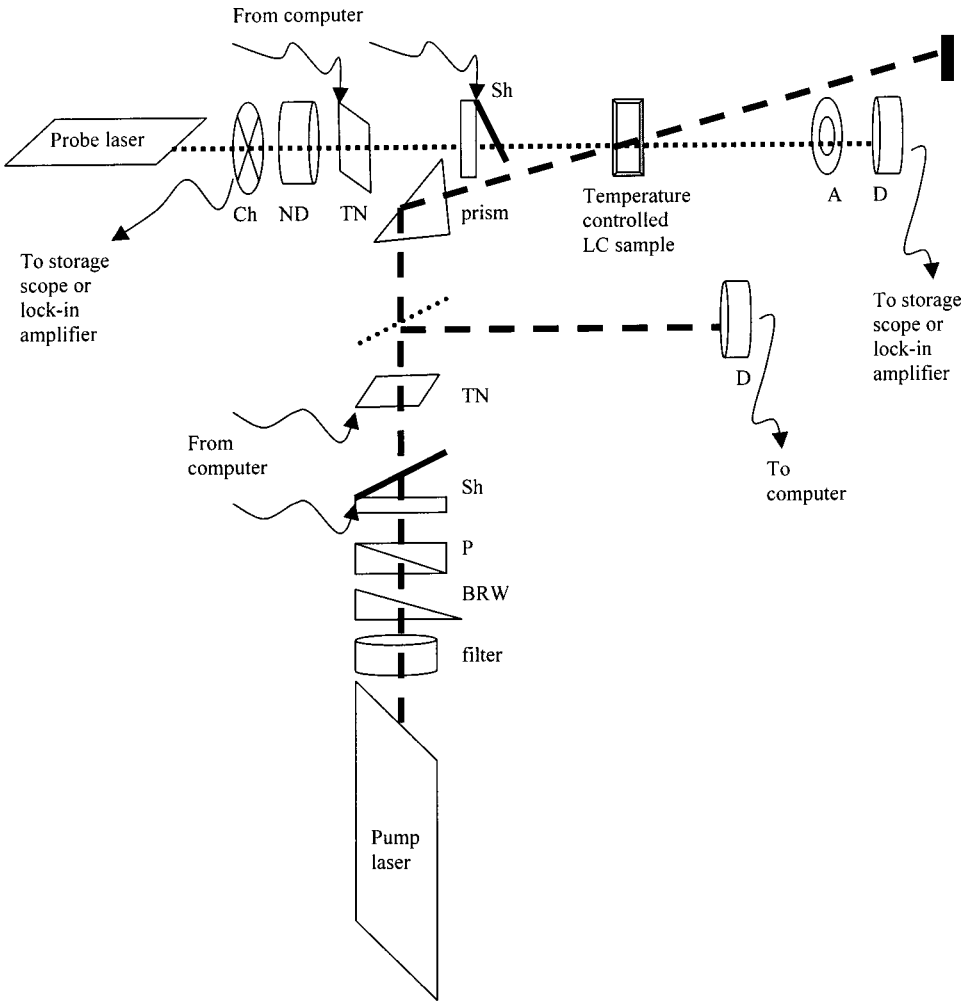

FIG. 1. Experimental setup. Ch—chopper, ND—neutral density filter, TN—twisted nematic cell, Sh—shutter, A—aperture, D—detector, p—polarizer, and BRW—birefringent wedge.

The dye DR-13 has a significantly shorter relaxation time than methyl red and DO3. In this case, a chopper replaced the shutter for the pump beam. The storage scope was set in averaging mode. While this method allowed for the measurement of the relaxation time for DR-13 in the liquid crystal host, saturation intensities could not be attained. Measurements were made for all three dyes at temperatures ranging from about 20 to 55 °C. In the liquid crystal E63, these measurements were done in 5° increments. In the liquid crystal 8CB, 1° increments were necessary as the smectic/

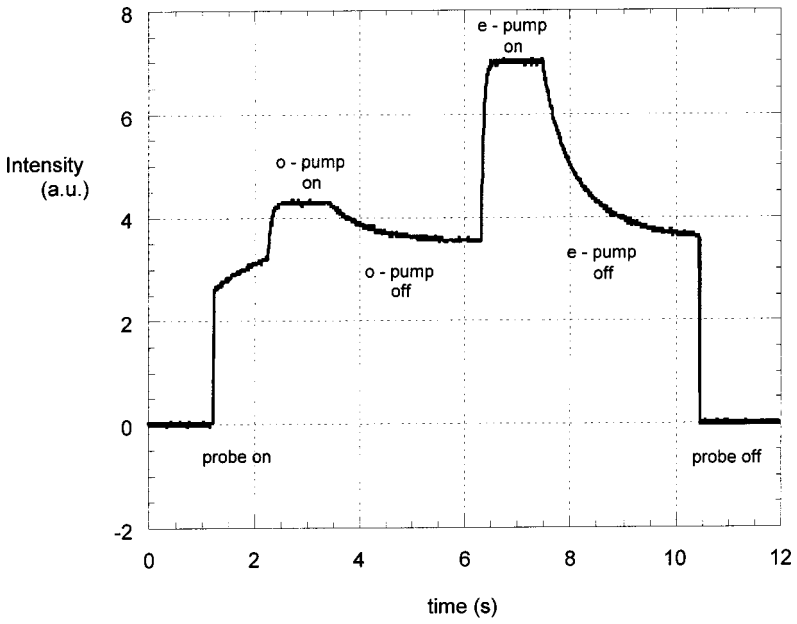

FIG. 2. Probe intensity vs time during sequence of pump switches.

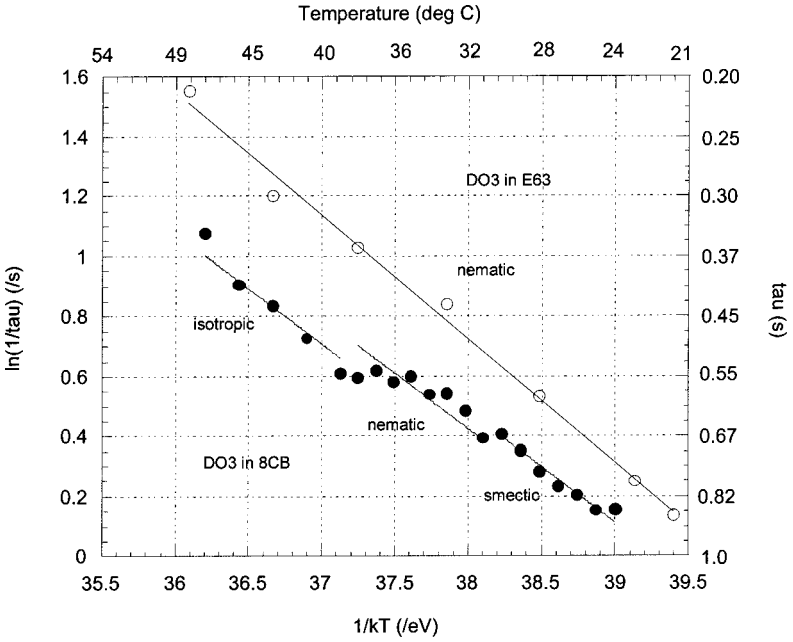

FIG. 3. Arrhenius plot; $\ln(1/\tau)$ versus $1/kT$. DO3 in 8CB (solid circles) and E63 (open circles).

nematic transition occurred at around 32 °C and the nematic/isotropic transition occurred at around 40 °C.

To determine the saturation intensity for methyl red and DO3, the probe absorbance was measured for several pump intensities. In this case, the probe was chopped, and the signal sent to a lock-in amplifier. This was done in 8CB in the smectic, nematic, and isotropic phases. In E63, where there is only a nematic phase, the measurements were made at room temperature.

IV. RESULTS AND DISCUSSION

A. Relaxation measurements

Figure 3 shows characteristic Arrhenius plots of $\ln[1/\tau]$ (τ being the measured relaxation time) verses $1/kT$, in this case for the dye DO3 in 8CB and E63. The slope of the curve is the barrier potential, E_A, and the intercept is $\ln[A]$ (i.e., $1/\tau = A \exp[-E_A/kT]$). Fit parameters are given in Table I. While it is possible that the barrier potential for isomerization may be slightly different in the three different phases of 8CB, such differences are smaller than the uncertainty in the measurement. In other words, it appears as though the phase of the liquid crystal does not have a significant effect on the height of the barrier potential. An average barrier potential was calculated and used to determine the pre-exponential factors for the dyes in each of the three phases. Inspection of Fig. 3 indicates that this method is reasonable. These fits show that the potential barrier to *cis-trans* isomerization is of the same order of magnitude for each of the three dyes, c.f. Table I. This indicates that the relatively high rate of isomerization for DR13, two orders of magnitude faster than either DO3 or methyl red, cannot be explained by differences in the barrier potential. Both in E63 and 8CB, DR13 and DO3 have comparable barrier potentials, whereas methyl red has the lower barrier potential. The fact that the relative isomerization rates are not explained by any differences in the barrier potentials is even more apparent when considering that methyl red, with the lowest barrier potential, is not the fastest to isomerize.

Any significant difference in isomerization rates is found in the pre-exponential factors shown in Table I. The low pre-exponential factor for methyl red compensates for its lower-energy barrier, while the high pre-exponential factor for DR13 is responsible for its fast isomerization rates. In addition, it can be seen in Fig. 3 and Table I that in 8CB the pre-exponential factor is slightly smaller in the isotropic phase than in the nematic phase. The difference, however, while systematic for all three dyes, is on the order of 10%. This suggests that in the isotropic phase, there is a small

TABLE I. Fit parameters for the Arrhenius plot of the inverse relaxation times.

Dye	Liquid crystal	Pre-exp factor, A, s^{-1} Smectic, nematic, isotropic Nematic	Energy barrier E_A (eV)	Relaxation time at 28.5 °C, s
Methyl	8CB	1.2×10^3, 1.2×10^3, 1.1×10^3	0.17	0.51
red	E63	3.4×10^2	0.15	0.80
DO3	8CB	2.1×10^6, 2.0×10^6, 1.8×10^6	0.37	0.75
	E63	1.3×10^7	0.41	0.59
DR13	8CB	1.2×10^8, 1.3×10^8, 1.2×10^8	0.33	2.7×10^{-3}
	E63	2.4×10^9	0.40	1.6×10^{-3}

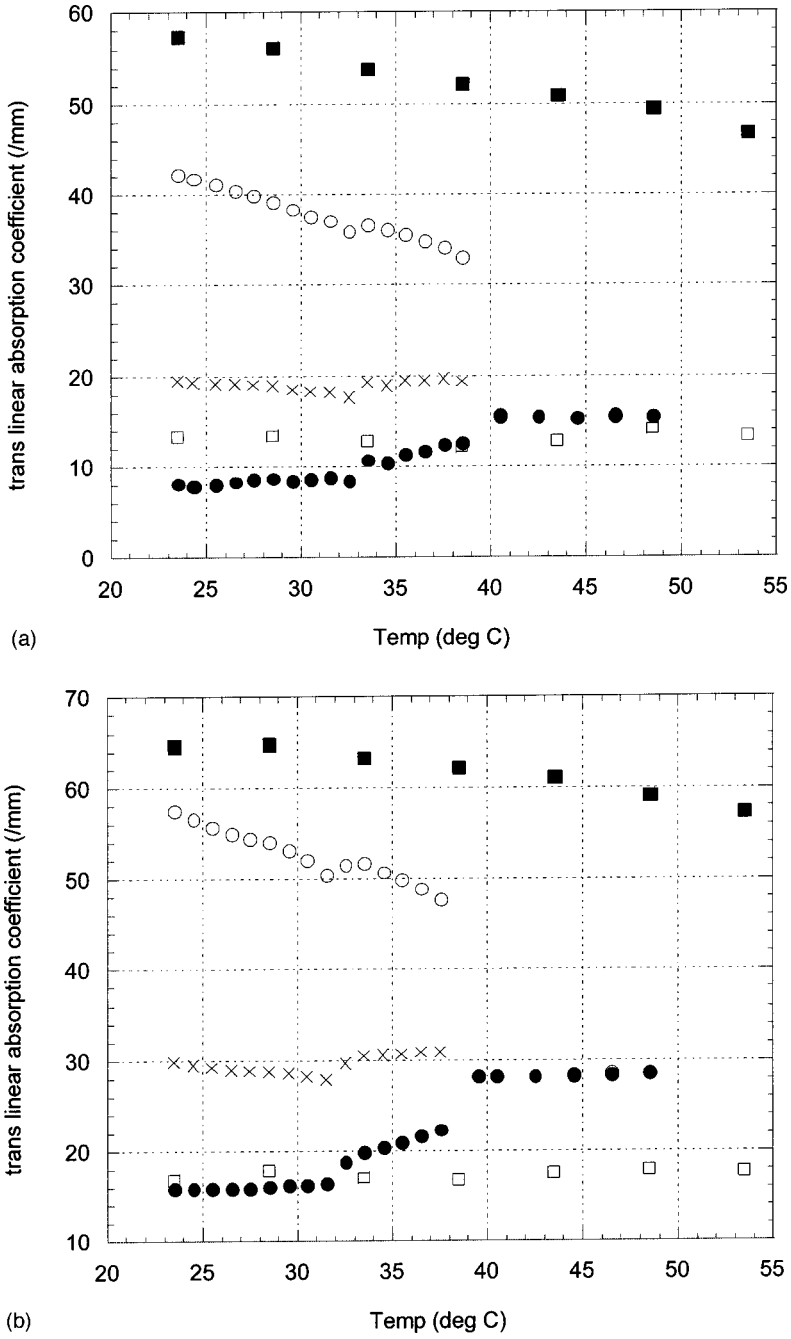

FIG. 4. (a) Linear absorption coefficient vs temperature: DO3 in 8CB: Open circles—α_{Te}, solid circles—α_{To}, and ×'s—$\alpha_{\text{average}}=(\alpha_{Te}+2\alpha_{To})/3$. DO3 in E63: Solid squares—α_{Te} and open squares—α_{To}. (b) Linear absorption coefficient vs temperature: Methyl red in 8CB: Open circles—α_{Te}, solid circles—α_{To}, and ×'s—$\alpha_{\text{average}}=(\alpha_{Te}+2\alpha_{To})/3$. Methyl red: Solid squares—α_{Te} and open squares—α_{To}.

amount of hindrance to isomerization, perhaps mechanical, that does not exist in the nematic phase.

The pre-exponential factor just discussed is determined by the shape of the potential curve along the reaction coordinate and by the ''friction'' experienced by the dye during isomerization.[12] These results indicate that this friction, which should be inversely proportional to the isomerization time in the absence of a barrier, does not necessarily scale with the viscosity of the liquid crystal host. Consider that for DR13 and DO3 the pre-exponential factor is larger in E63 than it is in 8CB, whereas for methyl red it is smaller. It is about 20 times larger for DR13, and about 6.5 times greater for DO3. But the pre-exponential factor for methyl red in E63 is only 28% of that in 8CB. Similarly, the energy barrier to isomerization for DR13 and DO3 is greater in E63 than it is in 8CB, whereas the opposite appears to be true for methyl red. In E63, the energy barrier is about 21% greater than it is in 8CB. For DO3, the energy barrier in E63 is about 11% greater than that in 8CB. And for methyl red, the energy barrier in E63 is about 12% less in E63 than in 8CB. Considering that the viscosities of E63 and 8CB are comparable, it must be concluded that the barrier shape is primarily responsible for these differences in the pre-exponential factor.[13] However, any conjecture beyond this is outside the scope of the present study.

B. Saturation measurements

Figures 4(a) and 4(b) show the linear absorption coefficients for the *trans* isomers of the dyes DO3 and methyl red,

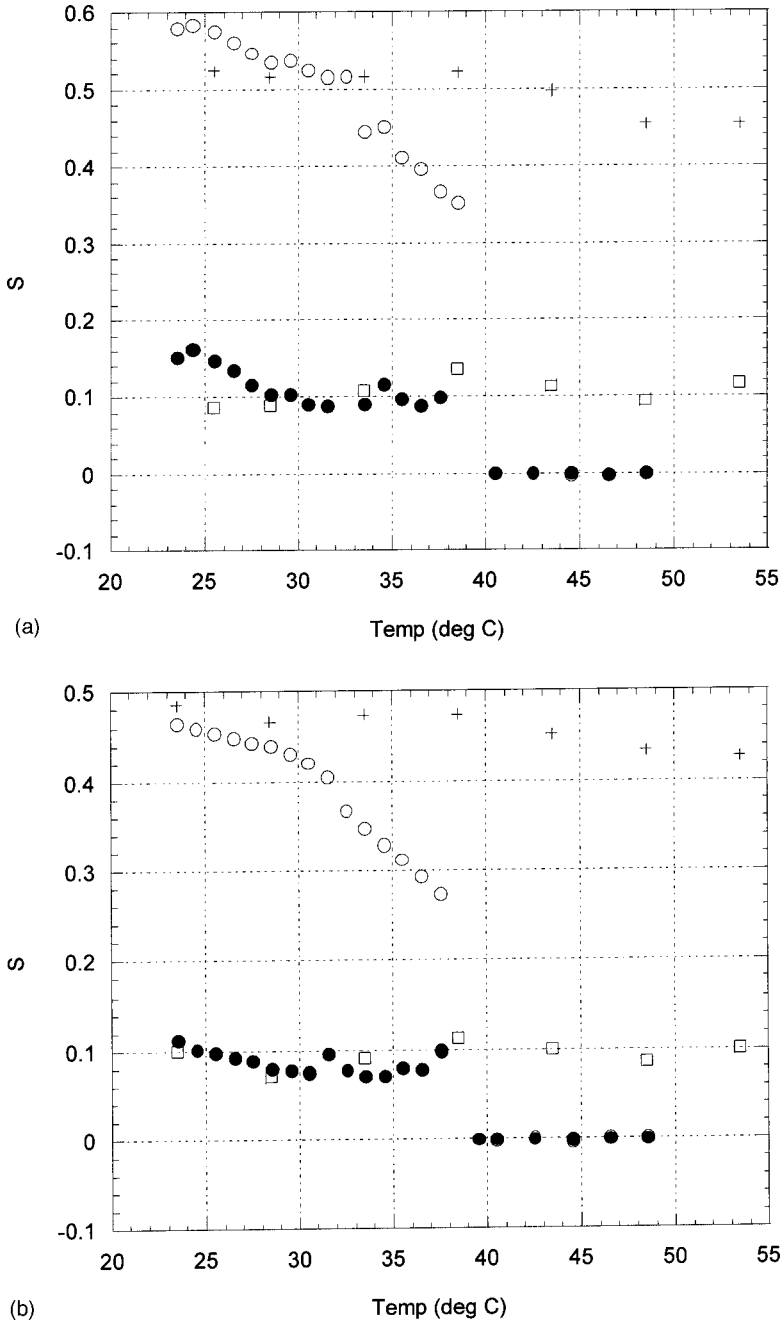

FIG. 5. (a) Order parameter vs temperature: DO3 in 8CB, open circles—*trans* and solid circles—*cis*, and in E63, +'s—*trans* and open squares—*cis*. (b) Order parameter vs temperature: Methyl red in 8CB, open circles—*trans* and solid circles—*cis*, and in E63, +'s—*trans* and open squares—*cis*.

respectively. In the plots of Figs. 4(a) and 4(b), the orientational average of the absorption coefficients, $(2\alpha_o+\alpha_e)/3$, is shown for 8CB also. Any change in this factor reflects variations in the density of the host and in local field correction.[14] At the phase transitions, discontinuities are observed. Interestingly, the average increases at the smectic–nematic transition, while it decreases at the nematic–isotropic transition. The average values measured in the smectic phase are rather close to the isotropic values; possibly the changes in local field correction and in density cancel each other.

In Fig. 5, the dichroism is shown, characterized by a ''dye order parameter,'' defined as

$$S=\frac{\alpha_e-\alpha_o}{\alpha_e+2\alpha_o}. \tag{12}$$

As can be seen from Fig. 5, the *trans* isomer has a relatively high dye order parameter in the liquid-crystalline phases, and its temperature dependence resembles that of the order parameter of the host.[15]

The *cis* absorption coefficients were evaluated from pump–probe experiments, using Eq. (9). In Fig. 5, the dye order parameter of the *cis* component is shown also. Although it is essentially smaller than that of the *trans* component, it still has a finite positive value in the liquid-crystalline phases, indicating a certain order of the *cis* molecules. The small value of the dichroism can have two origins. First, the angle between the transition dipole moment and the ''long axis'' (defined, e.g., as the axis with the smallest moment of inertia) can be much larger in the *cis* configuration than in the *trans*. Second, the guest–host interaction may be much

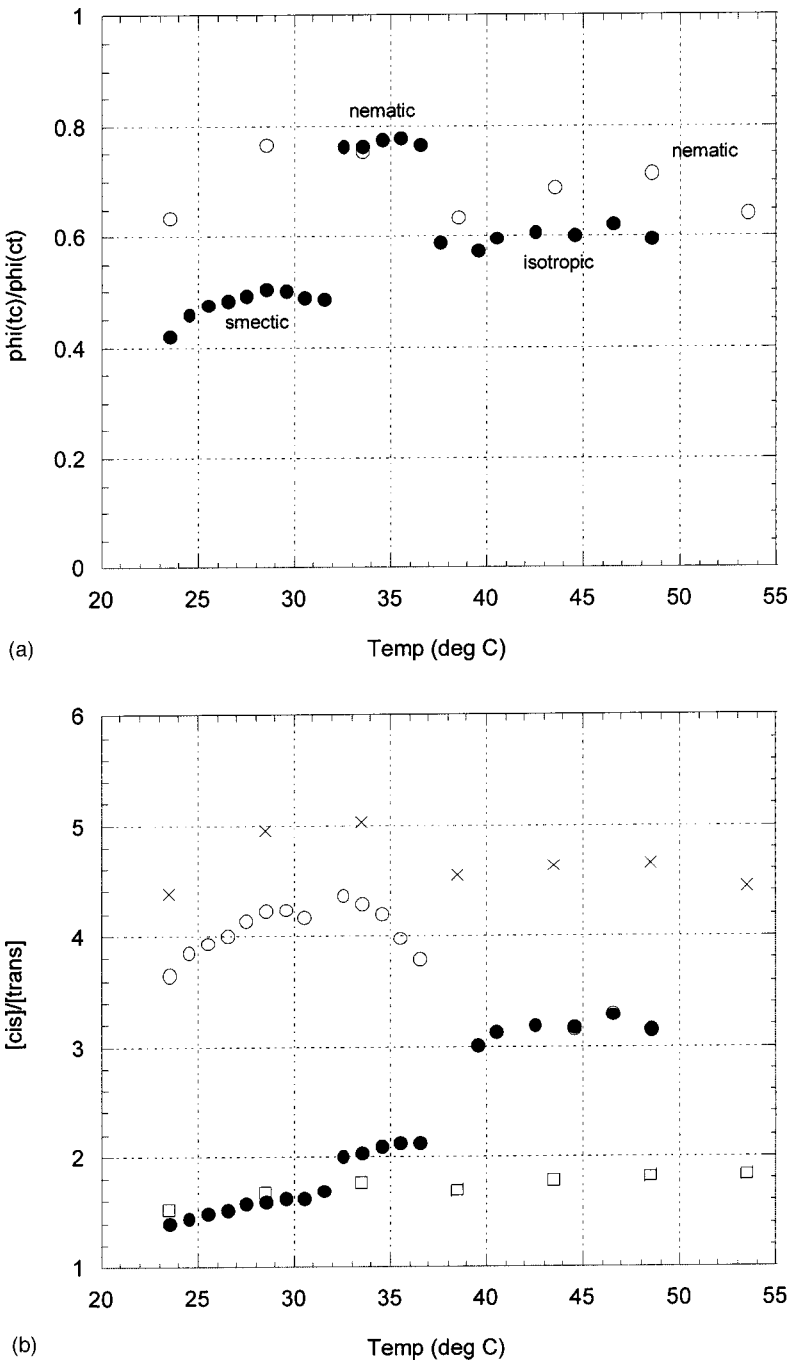

FIG. 6. (a) Quantum efficiency ratio vs temperature: DO3 in 8CB (solid circles) and in E63 (open circles). (b) Saturated concentration ratio, [*cis*]/[*trans*], vs temperature: DO3 in 8CB, open circles—*e* pump and solid circles—*o* pump, and in E63, ×'s—*e* pump and open squares—*o* pump.

weaker for the V-shaped *cis* isomer than for the *trans* isomer, which has a similar shape as the host molecules. As a consequence, the *trans* isomer can be aligned more effectively than the *cis* one. The dye order parameter of the *cis* component of both dyes correlates with the liquid-crystalline order in the smectic phase, but is more or less constant in the nematic phase.

In Figs. 6(a) and 6(b) the quantum efficiency ratio and the saturated [*cis*]/[*trans*] ratios are shown respectively, for the dye methyl red. The results obtained for DO3 are qualitatively similar to that of methyl red. It is important to note that Fig. 6(b) shows the photoinduced steady-state ratio [*cis*]/[*trans*], determined from the saturated [*cis*]/[*trans*] ratio using Eq. (5), to be dependent on the pump polarization in the liquid-crystalline phases.

As discussed in Sec. II, these quantities cannot be directly evaluated in the isotropic phase. In order to estimate their values in this phase, we assumed that isotropic absorption coefficient for the *trans* isomer is close to a weighted average of the *e* and *o* absorption coefficients in the smectic phase, and that this weighting holds for the *cis* isomer as well. With this assumption, an isotropic value of the *cis* linear absorption coefficient was calculated and used to estimate the quantum efficiency ratios, shown in Fig. 6(a), c.f. Eq. (9b). The saturated [*cis*]/[*trans*] ratio was then estimated using Eq. (5). This estimated ratio was found to be between the *e* and *o* values of the calculated values in the nematic phase, as shown in Fig. 6(a). As a second possibility, we determined the isotropic absorption coefficient for the *trans* isomer as a weighted average of the *e* and *o* absorption

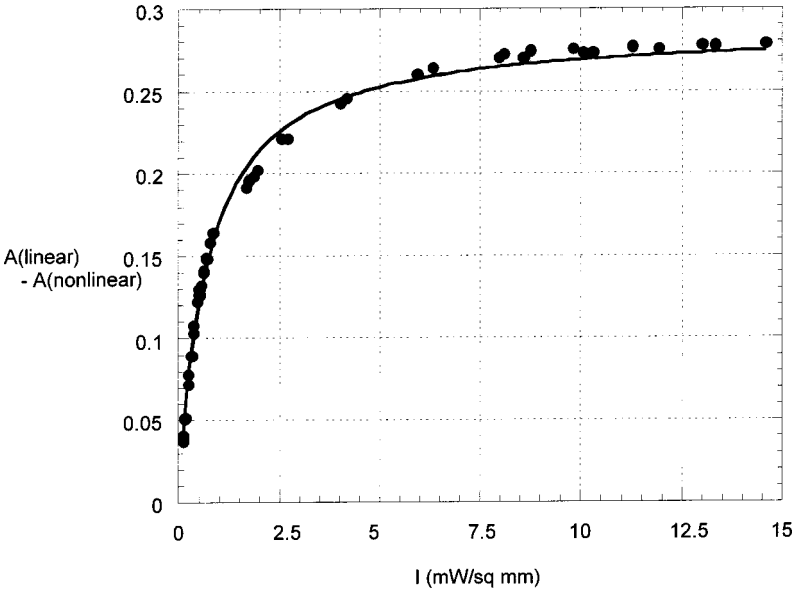

FIG. 7. Example of the difference between the linear and nonlinear absorbances vs pump intensity.

coefficients near the nematic–isotropic transition, and used this weighting to calculate the isotropic absorption coefficient of the *cis* isomer. Using this assumption, for both dyes in the isotropic phase, the estimated quantum flux ratios were about 3.3 times greater and the saturated [*cis*]/[*trans*] ratios were approximately 2 times greater than that using the first method. The saturated [*cis*]/[*trans*] ratios calculated in this manner were higher than either the *e* or the *o* values in the nematic phase. Although the situation depicted in Fig. 6(b), based on our first conjecture, seems to be more plausible, the second possibility cannot be excluded. Clearly, there is a certain amount of ambiguity in determining these parameters in the isotropic phase.

It can also be seen in Figs. 6 that in E63, both the quantum efficiency ratio and the saturated [*cis*]/[*trans*] ratios are relatively independent of temperature. This is true for both dyes. The quantum efficiency ratio, Φ_{TC}/Φ_{CT}, was found to be around 0.3 for DO3 and 0.7 for methyl red. For DO3, the saturated [*cis*]/[*trans*] ratios for the *e* and *o* pumps, respectively, were 1.2 and 0.4, whereas for methyl red they were 4.7 and 1.7.

Figure 6(b) also shows the *e* pumped saturated [*cis*]/[*trans*] ratio decreasing with temperature in the nematic phase of 8CB, but not in the nematic phase of E63. The decreasing *trans* absorption coefficients with temperature, along with the increasing in the *cis* absorption coefficients in 8CB, c.f. Fig. 4, is directly responsible for this. Smaller *trans* absorption coefficients and larger *cis* absorption coefficients translate directly into smaller [*cis*]/[*trans*] ratios. It is also possible, although presently not verifiable; that the entropy of the *trans* isomer in the nematic phase might be increasing with temperature while the entropy of the *cis* isomer remains relatively constant, as indicated by the dye order parameters. Such an increase in the entropy difference might possibly balance the positive energy difference resulting in temperature independent quantum efficiency ratios in the nematic phase of 8CB.

C. Saturation intensities and absolute values of the quantum efficiencies

Figure 7 shows an example of the difference between the linear and nonlinear absorbance as a function of pump intensity, in this case for DO3 in 8CB. The data were fit to Eq. (11) by varying the saturation intensity to minimize the difference between the left-and right-hand sides. The fit values for the saturation intensities are given in Table II. From these values it can be seen that in both the smectic and nematic phases of the liquid crystal host, the saturation intensity for ordinarily polarized light is about twice that of the extraordinarily polarized light. In the liquid-crystalline phases of 8CB, the saturation intensities for both dyes are comparable. In the isotropic phase of 8CB and in E63, the saturation intensity for methyl red is less than half that of DO3.

The saturation intensities for both DO3 and methyl red are quite small, in all cases, much less than 1 mW/mm^2. Saturation, however, does not occur until the intensity is somewhat higher, in most cases greater than 5 mW/mm^2. The reason for this is that as the light propagates through the sample, it is attenuated. At the point where the light intensity drops below the saturation intensity, the dye will no longer saturate.

Assuming the saturation intensities to be relatively con-

TABLE II. Saturation intensities.

Dye/Liquid crystal	Temperature (°C)	I_S^e (mW/mm^2)	I_S^o (mW/mm^2)
	27 (smectic)	0.10	0.20
DO3/8CB	37 (nematic)	0.14	0.27
	47 (isotropic)	0.43	0.43
DO3/E63	25 (nematic)	0.14	0.24
	27 (smectic)	0.14	0.29
Methyl red/8CB	37 (nematic)	0.15	0.30
	47 (isotropic)	0.19	0.19
Methyl red/E63	25 (nematic)	0.07	0.12

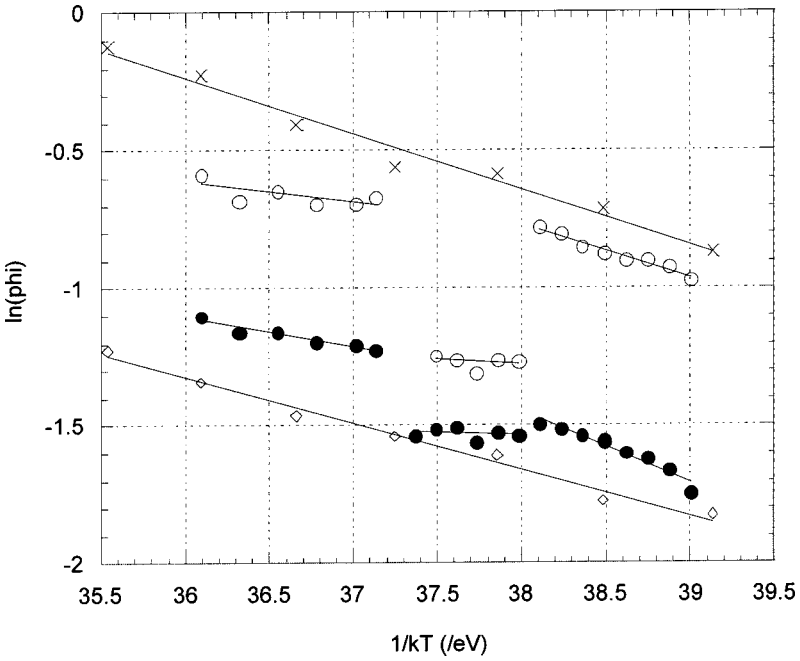

FIG. 8. Methyl red—Quantum efficiency vs $1/kT$. 8CB: Open circles—Φ_{CT} and solid circles—Φ_{TC}. E63: $\times$'s—Φ_{CT} and open diamonds—Φ_{TC}.

stant within a liquid crystal phase, the quantum efficiencies can be calculated,

$$\Phi_{TC}=N\left[I_S^i\alpha_T^i\frac{\tau}{h\nu}\left(1+\frac{\sigma_C^i}{\sigma_T^i}\frac{\Phi_{CT}}{\Phi_{TC}}\right)\right]^{-1}. \tag{13}$$

The values of $\ln[\Phi]$ for methyl red are shown in Fig. 8 as a function of $1/kT$. Methyl red DO3 shows similar results. These values may be subject to a systematic error, as they are based on the determination of the dye number density, N, from the mass fraction of dye and the density of the liquid crystalline host. However, the trends exhibited in Fig. 8 should be independent of such an error. Within a specific liquid crystal phase, the linearity of $\ln[\Phi]$ with $1/kT$ indicates that these quantum efficiencies follow a Boltzmann-type distribution. It shows that the *cis* to *trans* quantum efficiencies and the *trans* to *cis* quantum efficiencies tend to increase with temperature within that phase. Yet, in 8CB the quantum efficiency, Φ_{CT}, in the smectic phase is greater than that in the nematic phase, even though the smectic phase exists at lower temperatures. This is true for both dyes. In addition, in both the smectic and nematic phases, Φ_{CT} is always greater than Φ_{TC}. Figure 8 also indicates that the temperature dependence of Φ_{TC} in the nematic phase of 8CB tends to be weak.

The quantum efficiencies in the isotropic phase were estimated based on the assumptions discussed in Sec. IV B where the smectic absorption coefficients were used to calculate the isotropic absorption coefficients and estimate the quantum efficiency ratio, c.f. Fig. 6(a). Had the nematic absorption coefficients been used, Φ_{CT} would have been about 2.8 times smaller and Φ_{TC} would have been about 20% greater.

V. CONCLUSIONS

In comparing dye properties in the smectic, nematic, and isotropic phases, several items stand out. It is quite clear that the barrier to *cis-trans* isomerization is relatively unaffected by the liquid-crystalline phase. Yet, there is some additional hindrance to isomerization in the isotropic phase, indicating a slight increase in ''solvent friction.'' Regarding dye anisotropy, our results show that the dye order parameter for the *cis* isomer is not strongly dependent on the liquid-crystalline phase, whereas the opposite is true for the *trans* isomer. As discussed, this suggests that the dye order parameter for the *trans* isomer is a reasonably good measure of the liquid-crystalline order. While this order varies insignificantly in nematic E63, that is not the case for 8CB, where in the nematic phase the order changes most dramatically. Finally, our results also indicate that the quantum efficiencies for *cis-trans* isomerization and the saturated [*cis*]/[*trans*] ratios are dependent on the liquid-crystalline phase.

ACKNOWLEDGMENTS

The work was supported by the Copernicus Grant ''Photonic Devices: New Liquid Crystalline Materials'' IC 15-CT98-0806 and by the Hungarian Research Grant (No. OM-00224/2001). One of the authors (D.S.) would also like to acknowledge the Hungarian–American Fulbright Commission for its support.

APPENDIX: DERIVATION EQ. 11 FOR NONLINEAR ABSORBANCE

Equation (11) is derived by combining Eqs. (10a) and (10b) with Eq. (4). In particular, inserting Eq. (4) into Eq. (10a), with some rearrangement of terms, gives

$$dI^m = -\alpha_T^m \left(1 - D^m \frac{X_S^i}{1 + I_S^i / I^i} \right) dz. \quad \text{(A1)}$$

From Eq. (10b), $dz = dI^i / \alpha_T^i (D^i X_{\text{eq}}^i - 1) I^i$. This combined with Eqs. (4) and (A1), and some algebraic manipulation, gives

$$dI^m = -\alpha_T^m dz - \frac{\alpha_T^m}{\alpha_T^i} \left(\frac{D^m X_S^i}{1 - D^i X_S^i} \right) \frac{dI^i}{\left(I^i - \dfrac{I_S^i}{D^i X_S^i - 1} \right)}. \quad \text{(A2)}$$

The integration of Eq. (A2) gives Eq. (11).

[1] T. Ikeda and O. Tsutsumi, Science **268**, 1873 (1995).
[2] A. G. Chen and D. J. Brady, Opt. Lett. **17**, 441 (1992).
[3] R. W. Folks, Y. A. Reznikov, L. Chen, A. I. Khiznyak, and O. Lavrentovich, Mol. Cryst. Liq. Cryst. **261**, 259 (1995).
[4] M. I. Barnik, A. S. Zolotko, V. G. Rumyantsev, and D. B. Terskov, Crystallogr. Rep. **40**, 691 (1995).
[5] I. Jánossy and L. Szabados, Phys. Rev. E **58**, 4598 (1998).
[6] K. Anderle, R. Birenheide, M. J. A. Werner, and J. H. Wendroff, Liq. Cryst. **9**, 691 (1991).
[7] S. Hilvsted, F. Andruzzi, C. Kulinna, H. W. Siesler, and P. S. Ramanujam, Macromolecules **28**, 2172 (1995).
[8] T. G. Pedersen and P. M. Johansen, Phys. Rev. Lett. **79**, 2470 (1997).
[9] T. G. Pedersen, P. M. Johansen, N. C. R. Holme, and P. S. Ramanujam, J. Opt. Soc. Am. B **15**, 1120 (1998).
[10] T. G. Pedersen, P. S. Ramanujam, and P. M. Johansen, J. Opt. Soc. Am. B **15**, 2721 (1998).
[11] I. Jánossy and L. Szabados, J. Nonlinear Opt. Phys. Mater. **7**, 539 (1998).
[12] H. A. Kramers, Physica, **7**, 284 (1940); S. Chandrasekhar, Rev. Mod. Phys. **15**, 1 (1943).
[13] S. P. Velsko, D. H. Waldeck, and G. R. Fleming, J. Chem. Phys. **78**, 249 (1983); R. F. Grote and J. T. Hynes, *ibid.* **73**, 2715 (1980); K. Kwac, S. Lee, and K. J. Shin, Bull. Korean Chem. Soc. **16**, 427 (1995).
[14] I. C. Khoo and S. T. Wu, *Optics and Nonlinear Optics of Liquid Crystals* (World Scientific, Singapore 1993), Chap. 1.
[15] S. Chandrasekhar, *Liquid Crystals* (Cambridge University Press, Cambridge, UK, 1992), Chap. 5.2.